Positive colossal magnetoresistance from interface effect in *p-n* junction of $La_{0.9}Sr_{0.1}MnO_3$ and $SrNb_{0.01}Ti_{0.99}O_3$

Kui-juan Jin,* Hui-bin Lu, Qing-li Zhou, Kun Zhao, Bo-lin Cheng, Zheng-hao Chen, Yue-liang Zhou, and Guo-Zhen Yang
Institute of Physics, Chinese Academy of Sciences, Beijing 100080, China
(Received 3 September 2004; revised manuscript received 14 December 2004; published 31 May 2005)

Different from the negative colossal magnetoresistance (CMR) of the $LaMnO_3$ compound family, a positive CMR has been discovered at low applied magnetic field and high temperature in the epitaxial *p-n* heterostructure we fabricated with Sr-doped $LaMnO_3$ and Nb-doped $SrTiO_3$ by laser molecular-beam epitaxy. The mechanism causing the unusual positive CMR is proposed as a interface effect, i.e., the creation of a space charge region at the interface with different electron filling in bands comparing to that in the homogeneous region in Sr-doped $LaMnO_3$. Other puzzling CMR features with bias voltage, temperature, and even composition are well explained by the present scenario.

DOI: 10.1103/PhysRevB.71.184428 PACS number(s): 75.47.Gk, 73.20.−r, 73.43.Qt

The hole doped manganese oxides of general formula $La_{1-x}B_xMnO_3$ (B=Ca, Sr, Ba, Pb) have remarkable interrelated structural, magnetic, and transport properties. In particular, they exhibit very large negative magnetoresistance (MR), called colossal magnetoresistance (CMR) which value is defined as $MR=(R_H-R_0)/R_0$, with R_H denoting the resistance under applied magnetic field H and R_0 being the resistance without a magnetic field. The phenomenon of CMR is currently of considerable interest because of their value in fundamental physics and their potential applications.[1,2] The understanding of the microscopic physics underlying the CMR properties is therefore fundamentally important. Though good results of negative MR have been reported in some magnetic tunnel junctions (MTJ),[1–4] positive MR was found in very few systems.[5–8] Although wide and intense studies on the spin polarization, transport property and photoelectron spectra of $La_{0.7}Sr_{0.3}MnO_3$ have been carried out, little has been done for lower doped material such as $La_{0.9}Sr_{0.1}MnO_3$ due to its properties being similar with but less remarkable than those of $La_{0.7}Sr_{0.3}MnO_3$ for bulk or thin film. However, by depositing hole doped $La_{0.9}Sr_{0.1}MnO_3$ (LSMO) on electron doped $SrNb_{0.01}Ti_{0.99}O_3$ (SNTO) as we will show later in this Letter, a property of positive CMR is created in the system at low magnetic field and high temperature. Our most recent results for positive CMR in a multilayer heterostructure have been reported.[7] Although substantial values of magnetoresistance (MR) are found for a variety of materials at low temperatures, and in high magnetic fields, useful devices must operate at higher temperature even near room temperature, and in modest fields of H being less than 0.1 T. Thus, it is highly desirable to find new materials and structures with a large MR ratio at high temperature and a low applied magnetic field. Positive CMR values of 10.6% in 5 Oe, 23.2% in 100 Oe at 290 K, 53.0% in 5 Oe, 80.0% in 100 Oe at 255 K was found in the LSMO/SNTO *p-n* junction we fabricated, which are the largest in all CMR values for high temperature reported previously, including those absolute values for negative CMR in a low field and high temperature for perovskite oxide as far as we know. On the other hand, it is understandable for certain MTJ to be with a positive MR property, if the tunnelling occurs between two magnetic materials with different spin carriers.[5] However, it is amazing and even seems incredible for a system with the structure consisting of a nonmagnetic material (SNTO) and a negative CMR material (LSMO) to arise as a positive CMR property. The physics origin causing this unusual phenomenon is proposed as the creation of the space-charge region where the t_{2g} spin-down ($t_{2g}\downarrow$) band is partially filled by electrons in LSMO. According to this scenario, the CMR dependence on the bias voltage, composition, and the temperature can also be explained qualitatively.

In order to fabricate a better oxide *p-n* interface, a computer-controlled laser molecular-beam epitaxy (laser MBE)[9] was used to deposit the LSMO/SNTO *p-n* junctions. The *p-n* junction was made by depositing 0.1 Sr-doped $LaMnO_3$ with the thickness of 4000 Å directly on 0.01 Nb-doped $SrTiO_3$ (001), as shown in the inset of Fig. 1. The fabrication was done under the following condition: laser (with wavelength of 308 nm, repetition rate of 2 Hz, and duration of 20 ns) energy density approximately being 1 J/cm^2, the substrate temperature of 630 °C, and oxygen pressure of 2×10^{-3} Pa being maintained during the deposition. The growth rate was ~13 Å/min for LSMO. An *in situ* reflection high-energy electron diffraction (RHEED) provided useful information on surface structure, morphology,

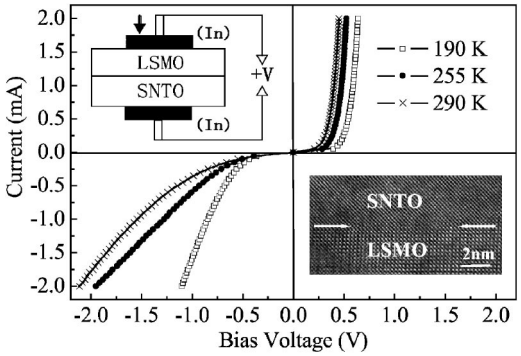

FIG. 1. The *I-V* curves of the $La_{0.9}Sr_{0.1}MnO_3/SrNb_{0.01}Ti_{0.99}O_3$ *p-n* junction without an applied magnetic field at various temperatures. Inset: schematic illustration of the *p-n* junction and the cross-sectional HRTEM image of the interface of the *p-n* junction.

and growth mode, and the oscillation of RHEED intensity was used to control the exact number of the deposited molecular layers. Our XRD $\theta-2\theta$ scan curve of the LSMO/SNTO *p-n* heterostructure shows that there exist only LSMO (00*l*) and SNTO (00*l*) peaks without any trace of other diffraction peak from impurity phase or randomly oriented grain, which means that the thin films of heterostructure are in single phase with *c* axis orientation. The cross-sectional high-resolution transmission electron microscopic (HRTEM) image in the inset of Fig. 1 also shows that the interface is perfectly oriented, and the epitaxial crystalline structure shows the axis of SNTO(001) being parallel to LSMO(001), and SNTO[100] being parallel to LSMO[100].

The current versus voltage ((*I-V*)) characteristics of the LSMO/SNTO junction without an applied magnetic field, measured with a pulse-modulated current source, showing the typical rectifying property of a *p-n* junction are shown in Fig. 1. The Ohmic contact between electrodes and the thin films was demonstrated by linear *I-V* curves, measured between the two electrodes on LSMO or SNTO thin film. The measurement was taken by a constant current with a step of 0.01 mA. The *I-V* behaviors of the LSMO/SNTO *p-n* junction in the magnetic field was measured in the temperature range of 190 to 290 K by a superconducting quantum interference device (SQUID, Quantum Design MPMS 5.5 T). A magnetic field perpendicular to the *p-n* interface and parallel to the current was applied. The influences of the magnetic field on the voltage of the *p-n* junction are more obvious with the negative bias than that with the positive bias, because the resistance at negative bias is larger than that at positive bias for the *p-n* junction. Figures 2(a)–2(c) show the dependence of the positive CMR as a function of negative bias voltage for the LSMO/SNTO *p-n* junction under an applied magnetic field varying from 5 to 1000 Oe at 190 K, 255 K, and 290 K, respectively. The character of increased MR with the increased magnetic field for various temperature in the high-temperature range in Fig. 2 clearly demonstrates a positive CMR feature of this structure. The maximum CMR value of each curve in Fig. 2 occurs at the voltage $|V|$ being in the range of 0.6 V to 0.8 V. Comparing Figs. 2(a)–2(c) plotted at different temperatures, we can see that for a constant magnetic field and a constant bias, most of the MR values increase with the temperature for 190 K and 255 K but decrease with the temperature for 255 K and 290 K. For example, with a magnetic field of 1000 Oe and a voltage of −0.8 V, the CMR value being 0.37 at 190 K is lower than that of 0.89 at 255 K, but the CMR value of 0.89 at 255 K is higher than that of 0.26 at 290 K. To see the doping dependence of the positive CMR, we elaborated the *p-n* junction with $La_{0.8}Sr_{0.2}MnO_3$ replacing $La_{0.9}Sr_{0.1}MnO_3$ in the same condition. The CMR measurement shows that the positive CMR of the $La_{0.8}Sr_{0.2}MnO_3/SrNb_{0.01}Ti_{0.99}O_3$ *p-n* junction is much lower than that of the $La_{0.9}Sr_{0.1}MnO_3/SrNb_{0.01}Ti_{0.99}O_3$ structure. These abnormal features are indeed puzzling.

To understand the physics inducing the abnormal positive CMR property of this *p-n* junction structure consisting of a nonmagnetic material (SNTO) and a negative CMR material (LSMO), we present our theoretical calculation for the band diagram of the interface region based on the band structures

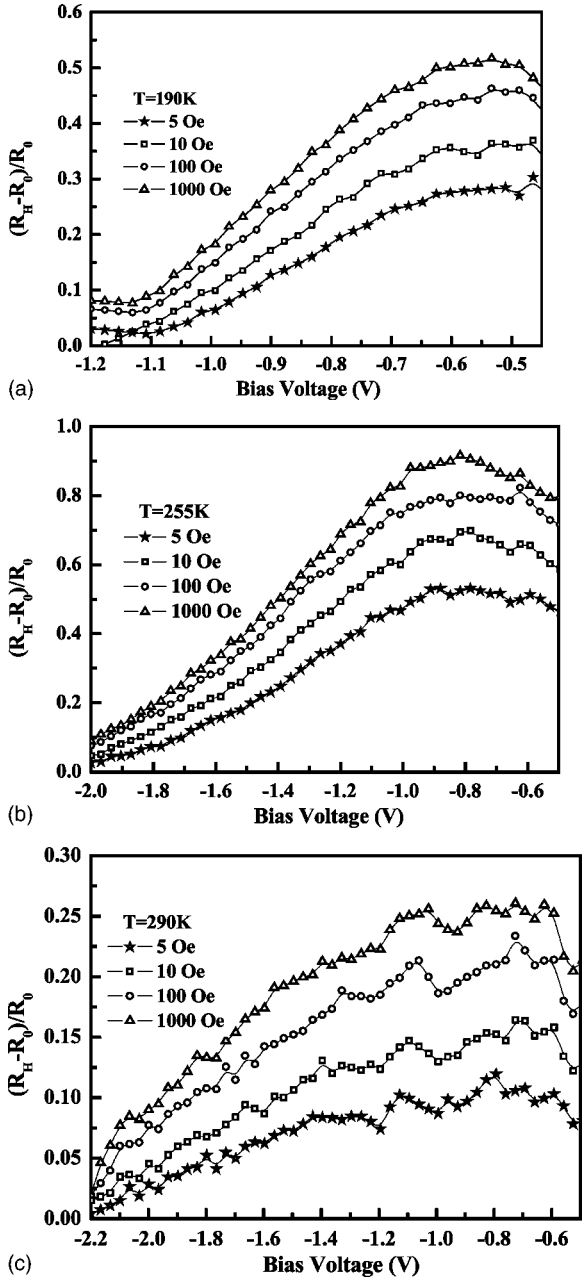

FIG. 2. The variation of MR values of the system with the negative bias voltage under several values of the applied magnetic field at the temperatures of 190 K (a), 255 K (b), and 290 K (c).

of LSMO and SNTO. In hole-doped manganistes LSMO, The five *d* orbitals are split by a cubic crystal field into three t_{2g} bands and two e_g bands. The degeneracy of the e_g band is further lifted by Jahn-Teller distortion into the e_g^1 band and the e_g^2 band. Furthermore, Hund's rule coupling removes the spin degeneracy in a magnetic state, as shown in the first region of Fig. 3. If SNTO is connected with LSMO in an applied magnetic field, the electrons from *n*-type SNTO will leak out into the adjacent *p*-type LSMO, even partially fill the t_{2g} spin-down ($t_{2g}\downarrow$) band after filling up the e_g^1 spin-up ($(e_g^1\uparrow)$) band of LSMO near the interface, then the Schottky barrier will be built up around the interface to stop the further leaking of electrons. On the LSMO side close to the

interface, a space-charge region where the electron density of states (DOS) is larger than that of the homogeneous regions of LSMO is created, as shown in Fig. 3. Therefore, the $t_{2g}\downarrow$ band edge is closer to the Fermi level in the space-charge region near the interface than that in the homogeneous region far from the interface. The existence of minority spin carriers in the hole-doped compound $La_{0.7}Sr_{0.3}MnO_3$ and in the MTJ system has been proposed.[5,10] Similar to previous work,[5] weak Hund's rule coupling (the splitting of $t_{2g}\uparrow$ and $t_{2g}\downarrow$ being smaller than the sum of the crystal field splitting energy between e_g and t_{2g} bands and Jahn-Teller splitting energy between two e_g bands) is proposed here as a hypothesis on which the existence of the minority spin carriers in the system is founded. For a system with a positive CMR, the $t_{2g}\downarrow$ band of the space-charge region has to be filled by some electrons. In other words, the creation of the space-charge region with electron filling in the $t_{2g}\downarrow$ band in LSMO is the origin causing the positive CMR in the heterostructure.

In order to show different regions in the structure in an applied magnetic filed, we plot Fig. 3(a) schematically and Fig. 3(b) resulting from our calculation for the system in equilibrium. In our calculation, Poisson's equation and the Boltzmann equation as follows was solved self-consistently for the equilibrium carrier densities ($p(x)$ for holes and $n(x)$ for electrons) and the electrostatic potential $\phi(x)$,

$$-\frac{d^2\phi(x)}{dx^2} = \frac{e}{\varepsilon}[p(x) - n(x) - N_A + N_D],$$

$$n(x) = N(T)\exp\left(-\frac{E_c - e\phi(x) - E_F}{k_B T}\right),$$

$$p(x) = P(T)\exp\left(-\frac{E_F - E_v + e\phi(x)}{k_B T}\right), \qquad (1)$$

where N_a and N_d denote the concentrations of the acceptor and the donor, which are taken from the Hall effect measurement as 1.0×10^{18} and 1.16×10^{19} cm^{-3}, respectively; $N(T)$ and $P(T)$ are effective densities for carriers that are the function of the effective mass and the temperature of materials. The effective masses for LSMO and SNTO are taken from Refs. 11 and 12. ε in the previous equation being a dielectric constant for LSMO or SNTO is taken from Refs. 11 and 13, and E_v and E_c denote the energies of the valence band and the conduction band, respectively. Region I in Fig. 3 denotes the LSMO homogeneous region far away from the interface, region II denotes the LSMO space-charge region close to the interface, region III is the SNTO space-charge region close to the interface, and region IV is the SNTO homogeneous region far away from the interface. In Fig. 3, E_F denotes the Fermi level in the system, E_g denotes the band gap between $t_{2g}\downarrow$ and $e_g{}^1\uparrow$, and ΔE is the energy deference between the $e_g{}^2\uparrow$ band edge and the $t_{2g}\downarrow$ band edge in LSMO. E_g is smaller than the band gap between the two bands of $e_g{}^\uparrow$ ($e_g{}^1\uparrow$ and $e_g{}^2\uparrow$) ($\approx$1.0 eV) due to the weak Hund's rule coupling and the Fermi level locates slightly above the valence band.[5,15–17] The Fermi level of homogeneous SNTO locates slightly above the bottom of Ti 3*d* conduction band being consistent with its metallic behavior concluded from our resistant versus temperature measurement, and the band gap of SNTO is taken as 2.8 eV, which is smaller than $SrTiO_3$[18–22] due to Nb doping.[14] The electrons in the $t_{2g}\downarrow$ band where the magnetization is antiparallel to the spin are minority spin carriers, and the electrons (or holes) in the $e_g{}^1\uparrow$ and the $e_g{}^2\uparrow$ band where the magnetization is parallel to the spin are majority spin carriers. The MR across such a *p*-*n* junction of the magnetic and a nonmagnetic compound depends on the relative spin orientation of electrons around the Fermi level in each region where the spin polarized carriers pass through.

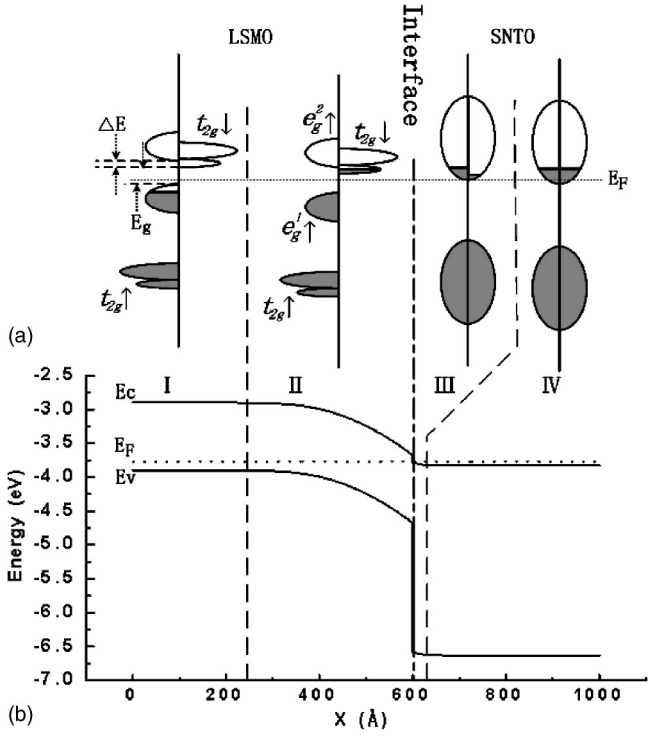

FIG. 3. The schematic DOS of the *p*-*n* junction (a), and the band diagram for each region (b) obtained by solving Eq. (1).

Now we focus on the positive CMR dependence on the applied negative bias V under which the Fermi level of region I (*p* side) is raised with respect to that of region IV (*n* side). We can approximately present the current decreasing part ΔI_+ (causing the positive MR) with the magnetic field H and the current increasing part ΔI_- (causing the negative MR) with H in the following way:

$$\Delta I_+ = I_+{}^0 - I_+{}^H \propto \mathrm{DOS}_I(E_{e^1\uparrow}) * \mathrm{DOS}_{II}(E_{t\downarrow}), \qquad (2)$$

$$\Delta I_- = I_-{}^H - I_-{}^0 \propto \mathrm{DOS}_I(E_{e^1\uparrow}) * \mathrm{DOS}_{II}(E_{e^2\uparrow}), \qquad (3)$$

where $\mathrm{DOS}_I(E_{e^1\uparrow})$ denotes the DOS at the electron filling level of the $e_g{}^1\uparrow$ band in region I, $\mathrm{DOS}_{II}(E_{e^2\uparrow})$ denotes the DOS of carries involved in the current in the $e_g{}^2\uparrow$ band in region II, and $\mathrm{DOS}_{II}(E_t\downarrow)$ denotes the DOS of carriers involved in the current in the $t_{2g}\downarrow$ band in region II under the bias *V*. Only if $\Delta I_+ > \Delta I_-$, the system can show a positive MR property. From above equations, it can be clearly seen that the electron filling in the $t_{2g}\downarrow$ band in region II is the origin causing the positive MR, and the competition between

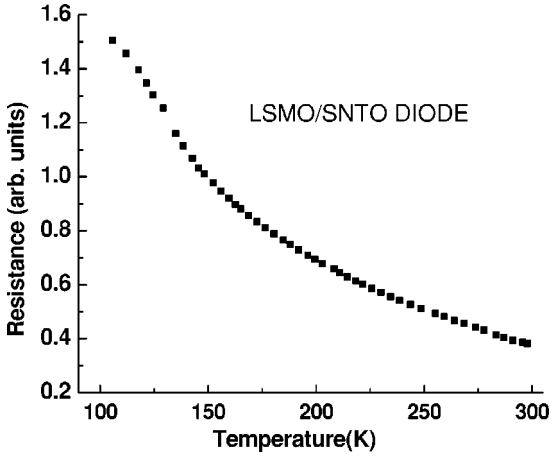

FIG. 4. The temperature dependence of the resistance for the heterostructure of $La_{0.9}Sr_{0.1}MnO_3$ and $SrNb_{0.01}Ti_{0.99}O_3$.

two sources of currents (Eq. (2) and (3)) plays a crucial role in the MR evolution with various measuring conditions of the system. At a very small bias $|V|$, the electrons in the region I hardly tunnel the barrier E_g to flow to the region II, thus almost no current flow in the system. This corresponds to what we observed at small negative bias voltage in Fig. 1. With the bias $|V|$ larger than a certain value, the electrons in the valence band of region I tunnel to the conduction band of region I, and current starts to flow in the system. But in this case, the majority channel of $e_g^{\,1}\uparrow$ has states available for most parts of the transport in region I, whereas the minority channel of $t_{2g}\downarrow$ dominates the transport in region II. With the increase of a magnetic field applied to the system, the spin polarization of the majority carrier in region I and the spin polarization of minority carrier in region II are both increased, thus less and less current can be carried from region I to region II due to the scattering between carriers with antiparallel spins; in other words, larger and larger resistance is caused in the system. Therefore, the positive MR is created at this bias voltage. With $|V|$ being larger than a certain value, the Fermi level of region I shifted up enough to reach the bottom of the $e_g^{\,2}\uparrow$ band of region II, so that the majority channel of $e_g^{\,2}\uparrow$ in region II starts to be available for transport, and thus the CMR value starts to decrease with the increase of $|V|$. This behavior of MR depending on the bias voltage agrees well with the phenomenon shown in Fig. 2. Furthermore, the maxima of CMR values in Fig. 2 occurring around the value of E_g verify our present scenario.

Comparing the two junctions of one with $La_{0.8}Sr_{0.2}MnO_3$ and the other one with $La_{0.9}Sr_{0.1}MnO_3$, the one with higher (0.2) Sr hole doping is with lower Fermi level. As the energy difference ΔE between the edges of $e_g^{\,2}\uparrow$ and $t_{2g}\downarrow$ bands is very small, the electrons in region II are mostly at the bottom of the $t_{2g}\downarrow$ band. Thus, the lowing of the Fermi level might cause great decreasing of the average DOS in the $t_{2g}\downarrow$ band of region II, as well as the positive CMR.

Now, Let us focus on the temperature dependence of the positive CMR. With the increased temperature, the electron filling of the $t_{2g}\downarrow$ band in region II increases, as well as the positive CMR in the system (190 K–255 K). If we keep increasing the temperature over a certain value, the filling of

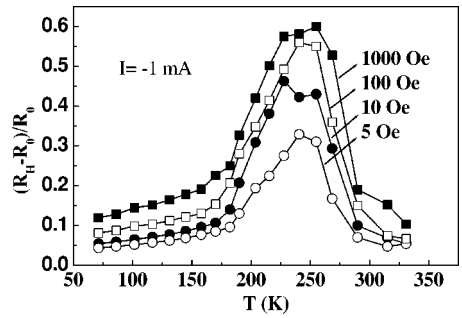

FIG. 5. The temperature dependence of the magnetoresistance ratio in the heterostructure of LSMO/SNTO.

electrons in region II could reach the band edge of $e_g^{\,2}\uparrow$ and the majority channel starts to be available, too, for the current. Therefore, with the increasing of temperature, the positive CMR decreases (255 K–290 K). In this scenario we can understand the positive CMR dependence on the temperature in Fig. 2.

The dependence of the resistance of the LSMO/SNTO heterostructure on the temperature between 90 K and 300 K we measured is plotted in Fig. 4, and the temperature dependence of the magnetoresistance ratio is shown in Fig. 5. The magnetization of the heterostructure for parallel and perpendicular fields, respectively, is plotted in Figs. 6(a) and 6(b). The corresponding magnetization for the substrate SNTO was also measured, and the results show that the magnetic momentum is two orders smaller than that of LSMO/SNTO heterostructure and almost keeps a constant for various temperature up to 300 K. Actually these values are comparable with the measuring background, which demonstrates that

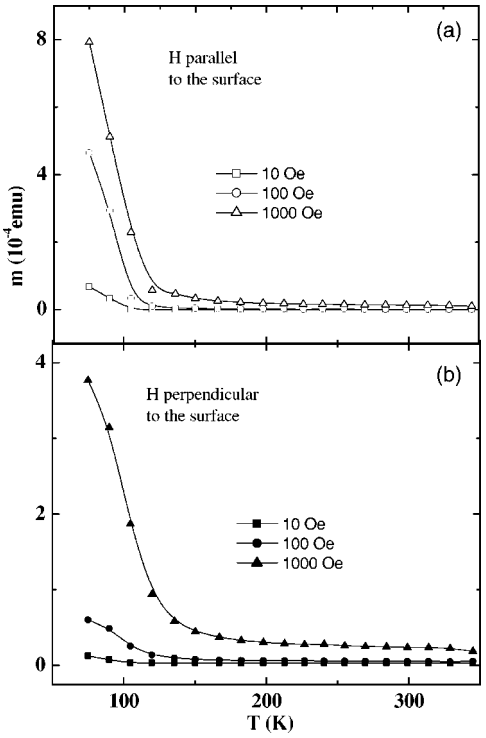

FIG. 6. The magnetic momentum of the heterostructure versus temperature.

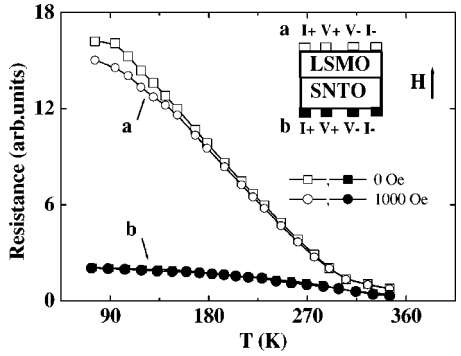

FIG. 7. Temperature-dependent resistance measured by using in-plane currents and the four-point geometry for LSMO (denoted by hollow symbols) and for SNTO (denoted by solid symbols).

SNTO can be taken as a nonmagnetic material. Figure 6 shows that there is no magnetic transition around 250 K, although the positive MR is the largest around 250 K. We can understand it in the following way. Although the density of states in the t_{2g} spin-down band in the interface region (which is sensitively dependent on temperature) plays a crucial role for the positive MR property in transport, it affects little the magnetization of the system that is contributed by the sum of contributions from the interface region and from the homogenous region of LSMO, as the depletion layer (the interface region) (20 nm thickness) is much thinner than the homogenous region (400 nm thickness) of LSMO, as shown in Fig. 3(b).

Furthermore, the resistance measurements used in-plane currents and the four-point geometry also have been carried out to clear out the properties of both components of the heterostructure. The results shown in Fig. 7 clearly demonstrate that the positive MR property indeed comes from the interface effect, as the LSMO film remains a negative CMR and SNTO is almost without any MR property in the system. Of course, the interface effect might also remain a little in the in-plane current measurement.

In the realistic system, the four regions are not clearly divided as to what are shown in Fig. 3(a), but merge one to the next smoothly from region I to IV. Thus, sharp interfaces between different regions (I and II, or III and IV) do not exist, but the origin of the positive CMR is in principle the same as we have presented above.

In summary, positive CMR properties of the LSMO/SNTO *p-n* junction have been reported and the origin of the puzzling phenomena has been proposed by the electron filling in the spin-down band in the space-charge region of LSMO close to the interface. Meanwhile, spin-up ($e_g^2\uparrow$) carriers of region II in transport plays a crucial role in the MR evolution at various measuring conditions. Moreover, the large sensitivity of the resistance to the magnetic field of the present structure in this Letter meets the high desire for the application of a large MR ratio in a low magnetic field and near room temperature. We believe the results and their physics origin we present in this Letter are important, not only from a practical viewpoint, but also as a potential of a new insight into the microscopic physics of the *p-n* junction consisting of the magnetic and nonmagnetic materials, since the value of the CMR is extremely sensitive to the band structure of the system. We hope the creation of the region with minority spin carriers in this structure can motivate studies on new structures of heterostructure (such as a junction consisting of a magnetic material and a semiconductor) and their amazing properties.

The authors would like to thank the National Natural Science Foundation of China for support.

*Corresponding author. Fax: 86-10-82648099; electronic address: kjjin@aphy.iphy.ac.cn

[1] C. Mitra, G. Kobernik, K. Dorr, K. H. Muller, L. Schultz, P. Raychaudhuri, R. Pinto, and E. Wieser, J. Appl. Phys. **91**, 7715 (2002);C. Mitra, P. Raychaudhuri, G. Kobernik, K. Dorr, K. H. Muller, L. Schultz, and R. Pinto, Appl. Phys. Lett. **79**, 2408 (2001).

[2] H. Dulli, P. A. Dowben, S.-H. Liou, and E. W. Plummer, Phys. Rev. B **62** R14 629 (2000);T. Obata, T. Manako, Y. Shimakawa, and Y. Kubo, Appl. Phys. Lett. **74**, 290 (1999);J. O'Donnell, A. E. Andrus, S. Oh. E. V. Colla, and J. N. Eckstein, *ibid.* **76**, 1914 (2000).

[3] J. Z. Sun, D. W. Abraham, K. Poche, and S. S. P. Parkin, Appl. Phys. Lett. **73**, 1008 (1998);W. J. Gallagher, S. S. P. Parkin, Y. Lu, X. P. Bian, A. Marley, K. P. Roche, A. Altman, S. A. Rishton, C. Jahnes, T. M. Shaw, and G. Xiao, J. Appl. Phys. **81**, 3741 (1997);J. Z. Sun, L. Krusin-Elbaum, P. R. Duncombe, A. Gupta, and R. B. Laibowitz, Appl. Phys. Lett. **70**, 1769 (1997).

[4] H. Tanaka, J. Zhang, and T. Kawai, Phys. Rev. Lett. **88**, 027204-4 (2002).

[5] C. Mitra, P. Raychaudhuri, K. Dorr, K. H. Muller, L. Schultz, P. M. Oppeneer, and S. Wirth, Phys. Rev. Lett. **90**, 017202 (2003).

[6] X. X. Zhang and J. M. Hernandez, Europhys. Lett. **47**, 487 (1999);P. Chen, D. Y. Xing, and Y. W. Du, Phys. Rev. B **64** 104402 (2001).

[7] H. B. Lu, G. Z. Yang, Z. H. Chen, S. Y. Dai, Y. L. Zhou, K. J. Jin, B. L. Cheng, M. He, L. F. Liu, Y. Y. Fei, W. F. Xiang, and L. Yan, Appl. Phys. Lett. **84**, 5007 (2004).

[8] K. Ghosh, S. B. Ogale, S. P. Pai, M. Robson, E. Li, I. Jin, Z. W. Dong, R. L. Greene, R. Ramesh, T. Venkatesan, and M. Johnson, Appl. Phys. Lett. **73**, 689 (1998).

[9] G. Z. Yang, H. B. Lu, Z. H. Chen, D. F. Cui, H. S. Wang, H. Q. Yang, F. Y. Miao, Y. L. Zhou, and L. Li, Sci. China, Ser. A: Math., Phys., Astron. **28**, 260 (1998).

[10] B. Nadgorny, I. I. Mazin, M. Osofsky, R. J. Soulen, Jr., P. Broussard, R. M. Stroud, D. J. Singh, V. G. Harris, A. Arenov, and Y. Mukovskii, Phys. Rev. B **63**, 184433 (2001).

[11] L. M. Wang, C.-c. Liu, H. C. Yang, and H. E. Horng, J. Appl. Phys. **95**, 4928 (2004).

[12] H. P. R. Frederikse, W. R. Thurber, and W. R. Hosler, Phys. Rev. **134**, A442 (1964).

[13] T. Tomio, H. Miki, H. Tabata, T. Kawai, and S. Kawai, J. Appl.

Phys. **76**, 5886 (1994);R. C. Neville, B. Hoeneisen and C. A. Mead, *ibid.* **43**, 2125 (1972).
[14] X. G. Guo, X. S. Chen, and W. Lu, Solid State Commun. **126**, 441 (2003).
[15] H. Y. Hwang, S.-W. Cheong, N. P. Ong, and B. Batlogg, Phys. Rev. Lett. **77**, 2041 (1996); Y. Okimoto, T. Katasufuji, T. Ishikawa, A. Urushibara, T. Arima, Y. Tokura, *ibid.* **75**, 109 (1995); J.-H. Park, C. T. Chen, S.-W. Cheong, W. Bao, G. Meigs, V. Chakarian, and Y. U. Idzerda, *ibid.* **76**, 4215 (1996).
[16] T. Saitoh, A. E. Bocquet, T. Mizokawa, H. Namatame, A. Fujimmori, M. Abbate, Y. Takeda, and M. Takano, Phys. Rev. B **51**, 13 942 (1995).
[17] A. Chainani, M. Mathew, and D. D. Sarma, Phys. Rev. B **47**, 15 397 (1993).
[18] X. G. Guo, X. S. Chen, and W. Lu, Solid State Commun. **126**, 441 (2003).
[19] A. Fujimori, I. Hase, M. Nakamura, H. Namatame, Y. Fujishima, Y. Tokura, M. Abbate, F. M. F. de Groot, M. T. Czyzyk, J. C. Fuggle, O. Strebel, F. Lopez, M. Domke, and G. Kaindl, Phys. Rev. B **46**, 9841 (1992).
[20] B. Reihl, J. G. Bednorz, and K. A. Müller, Phys. Rev. B **30**, 803 (1984).
[21] V. E. Henrich, G. Dresselhaus, and H. J. Zeiger, Phys. Rev. B **17**, 4908 (1978).
[22] Y.-w. Chung and W. B. Weissbard, Phys. Rev. B **20**, 3456 (1979).